Explicit Solutions for a Long-Wave Model with Constant Vorticity

Benjamin Segal*, Daulet Moldabayev†, Henrik Kalisch† and Bernard Deconinck*

Abstract

Explicit parametric solutions are found for a nonlinear long-wave model describing steady surface waves propagating on an inviscid fluid of finite depth in the presence of a linear shear current. The exact solutions, along with an explicit parametric form of the pressure and streamfunction give a complete description of the shape of the free surface and the flow in the bulk of the fluid. The explicit solutions are compared to numerical approximations previously given in [1], and to numerical approximations of solutions of the full Euler equations in the same situation [31]. These comparisons show that the long-wave model yields a fairly accurate approximation of the surface profile as given by the Euler equations up to moderate waveheights. The fluid pressure and the flow underneath the surface are also investigated, and it is found that the long-wave model admits critical layer recirculating flow and non-monotone pressure profiles similar to the flow features of the solutions of the full Euler equations.

1 Introduction

Background vorticity can have a significant effect on the properties of waves at the surface of a fluid [19,24,26,30,32,35]. In particular, in the seminal paper of Teles da Silva and Peregrine [31], it was found that the combination of strong background vorticity and large amplitude leads to a number of unusual wave shapes, such as narrow and peaked waves and overhanging bulbous waves. In the present contribution, we continue the study of a simplified model equation which admits some of the features found in [31]. The equation, which has its origins in early work of Benjamin [3], has the form

$$\left(Q + \frac{\omega_0}{2}u^2\right)^2 \left(\frac{du}{dx}\right)^2 = -3\left(\frac{\omega_0^2}{12}u^4 + gu^3 - (2R - \omega_0 Q)u^2 + 2Su - Q^2\right), \tag{1}$$

where we denote the volume flux per unit span by Q, the momentum flux per unit span and unit density corrected for pressure force by S, and the energy density per unit span by R. The gravitational acceleration is g and the constant vorticity is $-\omega_0$. The total flow depth as measured from the free surface to the rigid bottom is given by the function $u(x)$.

Equation (1) was recently studied in [1]. It was found that solutions of this equation exhibit similar properties as solutions of the full Euler equations displayed in [31]. In particular, in [1] an expression for the pressure was developed, and it was shown that the pressure may become non-monotone in the case of strong background vorticity. Indeed, it was shown in [1] that if

*Department of Applied Mathematics, University of Washington, Seattle, WA 98195-2420, USA
†Department of Mathematics, University of Bergen, Postbox 7800, 5020 Bergen, Norway

$|\omega_0|$ is big enough, the maximum fluid pressure at the bed is not located under the wavecrest. Such behavior is usually only found in transient problems (cf. [33]). Moreover in some cases, the pressure near the crest of the wave may be below atmospheric pressure.

The purpose of the present work is two-fold. First, we develop a method by which equation (1) can be solved *exactly*. The resulting solutions are compared to the the numerical approximations found in [1] and to some of the solutions of the full Euler equations from [31]. Secondly, more features of the solutions of (1) are discussed. Using a similar analysis as in [1], the streamfunction is constructed, and it is found that solutions of (1) may feature recirculating flow and pressure inversion. These features may have an impact on the study of sediment resuspension. Indeed, while it is generally accepted that the main mechanism for sediment resuspension is turbulence due to flow separation in the presence of strong viscous shear stresses [7,27,29], the strongly non-monotone pressure profiles exhibited by the solutions of (1) may represent a more fundamental mechanism for particle suspension than the viscous theory.

The geometric setup of the problem is explained as follows. Consider a background shear flow $U_0 = \omega_0 z$, where ω can be positive or negative (cf. Figure 1). Superimposed on this background flow is wave motion at the surface of the fluid. One may argue that the wave motion itself introduces variations into the shear flow due to the Stokes drift [16, 25]. However for very long waves, the Stokes drift can be compared to the Stokes drift in the KdV equation [5], and it becomes negligible in the long-wave limit. Moreover, as observed by a number of authors [3, 31, 32], a linear shear current can be taken as a first approximation of more realistic shear flows with more complex structures.

If it is assumed that the free surface describes a steady periodic oscillatory pattern, then the flow underneath the free surface can be uniquely determined [10, 23], even in the presence of vorticity. Thus for the purpose of studying periodic traveling waves, one may use a reference frame moving with the wave. This change of reference frame leads to a stationary problem in the fundamental domain of one wavelength. The incompressibility guarantees the existence of the streamfunction ψ and if constant vorticity $\omega = -\omega_0$ is stipulated, the streamfunction satisfies the Poisson equation

$$\Delta\psi = \psi_{xx} + \psi_{zz} = \omega_0, \text{ in } 0 < z < \eta(x) = \psi|_{z=\eta}. \tag{2}$$

As explained in [2,4], the three parameters Q, S and R are defined as follows. If $\psi = 0$ on the streamline along the flat bottom, then Q denotes the total volume flux per unit width given by

$$Q = \int_0^\eta \psi_z dz\,. \tag{3}$$

Thus Q is the value of the streamfunction ψ at the free surface. The flow force per unit width S is defined by

$$S = \int_0^\eta \left\{ \tfrac{P}{\rho} + \psi_z^2 \right\} dz, \tag{4}$$

and the energy per unit mass is given by

$$R = \frac{1}{2}\psi_z^2 + \frac{1}{2}\psi_x^2 + g\eta \text{ on } z = \eta(x)\,. \tag{5}$$

Finally, the pressure can be expressed as

$$P = \rho\Big(R - gz - \frac{1}{2}(\psi_x^2 + \psi_z^2) + \omega_0\psi - \omega_0 Q\Big), \tag{6}$$

It is well known that the quantities Q and S do not depend on the value of x [4]. Using the fact that S is a constant, the derivation of the model equation (1) can be effected by assuming that the waves are long, scaling z by the undisturbed depth h_0, x by a typical wavelength L, and expanding in the small parameter $\beta = h_0^2/L^2$. This yields (1) as an approximate model equation describing the shape of the free surface. In order to distinguish from the free surface η in the full Euler description, we call the unknown of equation (1) u which is an approximation of η. The derivation of (1) was given in [1, 4], where it was shown that (1) is expected to be valid as an approximate model equation describing waves on the surface of the shear flow if the wavelength is long compared to the undisturbed depth of the fluid. On the other hand, a detailed analysis of the derivation explained in [1, 4] shows that there are no assumptions on the amplitude of the waves. Thus at least formally, the model (1) can be expected to model waves of intermediate amplitude.

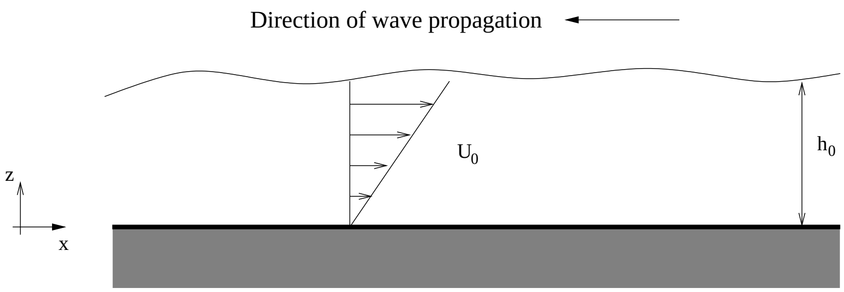

Figure 1: This figure shows the background shear flow $U_0 = \omega_0 z$. In the figure, ω_0 is positive, and the waves which are superposed onto this background current propagate to the left.

2 Explicit solutions

In order to obtain solutions of (1) given in explicit form, we apply the change of variables

$$\frac{dy}{ds} = \frac{du}{dx}\left(Q + \frac{\omega_0}{2}u^2\right),$$

$$y(s) = u(x).$$

This gives us a new equation for $y(s)$ in the form

$$\left(\frac{dy}{ds}\right)^2 = -3\left(\frac{\omega_0^2}{12}y^4 + gy^3 - (2R - \omega_0 Q)y^2 + 2Sy - Q^2\right), \tag{7}$$

and the relation

$$\frac{ds}{dx} = \frac{1}{Q + y^2\omega_0/2}. \tag{8}$$

Integrating (8) we have

$$x(s) = \int^s \left(Q + \frac{\omega_0}{2}y^2\right) d\xi - x_1. \tag{9}$$

where x_1 is a constant of integration, written explicitly for convenience. We want to solve (7) for $y(s)$ and plug our solution into (9). We notice that in the variables y and $\frac{dy}{ds}$ the equation describes an elliptic curve of genus one [14]. Hermite's Theorem [34, p. 394] states that for a uniform solution to exist we need $\int ds$ to be an abelian integral of the first kind. This condition is indeed satisfied and we proceed with using a birational transformation to put (7) in the standard Weierstraß form

$$\left(\frac{dy_0}{dx_0}\right)^2 = 4y_0^3 - g_2 y_0 - g_3, \tag{10}$$

where the transformation is given as

$$x_0 = -\frac{24(-2\sqrt{12}Q^2y^2\omega_0 - \sqrt{12}Qgy^3 + 4\sqrt{12}QRy^2 + 4\sqrt{12}Q^3 - 6\sqrt{12}QSy + 8Q^2\frac{dy}{ds} - 4\frac{dy}{ds}Sy)}{y^3},$$

$$y_0 = \frac{4(-Qy^2\omega_0 + 2Ry^2 + \frac{dy}{ds}\sqrt{12}Q + 6Q^2 - 6Sy)}{y^2}, \tag{11}$$

and g_2 and g_3 are the lattice invariants

$$g_2 = -768QR\omega_0 + 768R^2 - 1152Sg,$$

$$g_3 = 2048Q^3\omega_0^3 - 6144Q^2R\omega_0^2 - 6912Q^2g^2 \\ + 6144QR^2\omega_0 - 4608QSg\omega_0 + 2034S^2\omega_0^2 - 4096R^3 + 9216RSg.$$

It is well known that the solution to (10) is $y_0(x_0) = \wp(x_0 + c_0; g_2, g_3)$, where $\wp$ is the Weierstraß P function and c_0 is an arbitrary constant [6, 14]. We invert the birational transformation to determine the exact solution to (7) as

$$y(s) = \frac{A + B\wp'((s+c_0)/4; g_2, g_3) + C\wp((s+c_0)/4; g_2, g_3)}{\wp^2((s+c_0)/4; g_2, g_3) + D\wp((s+c_0)/4; g_2, g_3) + E},$$

with

$$A = -288Q^2g - 96Q\omega_0S + 192RS,$$
$$B = \sqrt{12}Q,$$
$$C = -24S,$$
$$D = 8Q\omega_0 - 16R,$$
$$E = 64Q^2\omega_0^2 - 64QR\omega_0 + 64R^2.$$

This gives us $u(x(s))$ in the form

$$u(x(s)) = \frac{A + B\wp'((s+c_0)/4; g_2, g_3) + C\wp((s+c_0)/4; g_2, g_3)}{\wp^2((s+c_0)/4; g_2, g_3) + D\wp((s+c_0)/4; g_2, g_3) + E}, \tag{12}$$

as a function of the parameter s. If we express $x(s)$ as a function of s, then we have a parametric representation for $u(x)$, the surface elevation. From (9) we have

$$x(s) = Qs - x_1 + \frac{\omega_0}{2}\int^s y^2(\xi)d\xi. \tag{13}$$

Expanding and simplifying $y(s)^2$ gives

$$y^2 = \frac{4B\wp^3 + C^2\wp^2 + (2AC - B^2g_2)\wp + (A^2 - B^2g_3)}{(\wp^2 + D\wp + E)^2} + \frac{2AB - 2BC\wp}{(\wp^2 + D\wp + E)^2}\wp', \tag{14}$$

making use of the shorthand $\wp = \wp((s+c_0)/4; g_2, g_3)$ and $\wp' = \wp'((s+c_0)/4; g_2, g_3)$. Plugging (14) into (13) and integrating gives

$$x(s) = Qs - x_1 + \omega_0 B \left[\frac{8(2A - CD)\arctan\left(\frac{D+2\wp}{\sqrt{-D^2+4E}}\right)}{(-D^2+4E)^{3/2}} + \frac{-4AD + 8CE + (-8A + 4CD)\wp}{(D^2 - 4E)(\wp^2 + D\wp + E)} \right]$$
$$+ \frac{\omega_0}{2} \int^s \frac{4B\wp^3 + C^2\wp^2 + (2AC - B^2 g_2)\wp + (A^2 - B^2 g_3)}{(\wp^2 + D\wp + E)^2} d\xi. \tag{15}$$

To evaluate the integral in (15) we let

$$m_1 = -\frac{D}{2} - \frac{\sqrt{D^2 - 4E}}{2},$$

$$n_1 = -\frac{D}{2} + \frac{\sqrt{D^2 - 4E}}{2},$$

denote the roots of $\wp^2 + D\wp + E = 0$. The integrand can be split into its components

$$\frac{4B\wp^3 + C^2\wp^2 + (2AC - B^2 g_2)\wp + (A^2 - B^2 g_3)}{(\wp - m_1)^2(\wp - n_1)^2} = \frac{J(m_1, n_1)}{(\wp - m_1)^2} + \frac{K(m_1, n_1)}{\wp - m_1} + \frac{J(n_1, m_1)}{(\wp - n_1)^2} + \frac{K(n_1, m_1)}{\wp - n_1},$$

with

$$J(m_1, n_1) = \frac{A^2 - B^2 g_3 + 2ACm_1 - B^2 g_2 m_1 + C^2 m_1^2 + 4B^2 m_1^3}{D^2 - 4E},$$

$$K(m_1, n_1) = \frac{-2A^2 + 2B^2 g_3 - 2ACm_1 + B^2 g_2 m_1 + 4B^2 m_1^3 - 2ACn_1 + B^2 g_2 n_1 - 2C^2 m_1 n_1 - 12B^2 m_1^2 n_1}{(4E - D^2)^{3/2}}.$$

Letting

$$\alpha = \wp^{-1}(m_1),$$
$$\beta = \wp^{-1}(n_1),$$

and

$$x_1 = -c_0 Q + x_2,$$

where x_2 is another arbitrary constant, we express $x(s)$ as

$$x(s) = Q(s + c_0) - x_2 + \omega_0 B \left[\frac{8(2A - CD)\arctan\left(\frac{D+2\wp}{\sqrt{-D^2+4E}}\right)}{(-D^2+4E)^{3/2}} + \frac{-4AD + 8CE + (-8A + 4CD)\wp}{(D^2 - 4E)(\wp^2 + D\wp + E)} \right]$$
$$+ 2\omega_0 \big[J(m_1, n_1) I_2((s + c_0)/4, \alpha) + K(m_1, n_1) I_1((s + c_0)/4, \alpha)$$
$$+ J(n_1, m_1) I_2((s + c_0)/4, \beta) + K(n_1, m_1) I_1((s + c_0)/4, \beta) \big], \tag{16}$$

where I_1 and I_2 come from [6] and [21] and are expressed as

$$I_1(u, \gamma) = \frac{1}{\wp'(\gamma)} \left[\log\left(\frac{\sigma(u - \gamma)}{\sigma(u + \gamma)}\right) + 2u\zeta(\gamma) \right],$$

$$I_2(u, \gamma) = \frac{\wp''(\gamma)}{\wp'^3(\gamma)} \log\left(\frac{\sigma(u + \gamma)}{\sigma(u - \gamma)}\right) - \frac{1}{\wp'^2(\gamma)} (\zeta(u + \gamma) + \zeta(u - \gamma)) - \left(\frac{2\wp(\gamma)}{\wp'^2(\gamma)} + \frac{2\wp''(\gamma)\zeta(\gamma)}{\wp'^3(\gamma)} \right) u.$$

Here ζ is the Weierstraß zeta function and σ is the Weierstraß sigma function. Thus we have $x(s)$ given in (16) and $u(x(s))$ given in (12) both as functions of s. This gives a parametric representation of our solution as a function of s

$$\begin{cases} y = u(x(s)), & \text{given in (12)}, \\ x = x(s), & \text{given in (16)}. \end{cases} \tag{17}$$

The approximation to the pressure given in [1] is

$$P = \rho \Bigg\{ R - gz - \frac{1}{2}\left(\frac{Q}{u^2} + \frac{\omega_0}{2}\right)^2 (z^2 u'^2 + u^2) + \frac{1}{2}\left(\frac{\omega_0}{6}u^3 - \frac{\omega_0}{2}z^2 u - \frac{2}{3}\omega_0 z^3 - \frac{Q}{3}u + z^2\frac{Q}{u}\right) \\ \times \left(2Q\frac{u'^2}{u^3} - u''\left(\frac{Q}{u^2} + \frac{\omega_0}{2}\right)\right) \Bigg\}. \tag{18}$$

This leads to a parametric representation of the pressure as a function of s

$$\begin{cases} y = P(u(x(s)), z), & \text{given in (18)}, \\ x = x(s), & \text{given in (16)}, \end{cases} \tag{19}$$

where z is the distance from the channel bed.

Finally, note that an expression for the streamfunction can be derived using the techniques of [1]. Since this was not done in [1], the derivation is outlined in the appendix for the sake of completeness. The expression for the streamfunction is

$$\psi = \frac{1}{2}z^2\omega_0 + z\left(\frac{Q}{u} - \frac{u\omega_0}{2} + \frac{Qu'^2}{3u} - \frac{Qu''}{6} - \frac{\omega_0 u^2 u''}{12}\right) - \frac{z^3}{6}\left(\frac{2Qu'^2}{u^3} - \frac{Qu''}{u^2} - \frac{\omega_0 u''}{2}\right), \tag{20}$$

which gives a parametric representation of the streamfunction as a function of s as

$$\begin{cases} y = \psi(u(x(s)), z), & \text{given in (20)}, \\ x = x(s), & \text{given in (16)}. \end{cases} \tag{21}$$

3 Matching the explicit solutions to previous works

First, we verify the explicit solutions found here and the numerical approximations given in [1] by comparing them to each other. Following the analysis of [1], we first note that (1) can be written in the form

$$u'^2 = \frac{\mathcal{G}(u)}{\mathcal{F}(u)}. \tag{22}$$

Letting Z_1, Z_2, m and M represent the roots of the numerator $\mathcal{G}$ on the right-hand side of (22) we write

$$\begin{aligned} \mathcal{G}(u) &= -3\left(\frac{\omega_0^2}{12}u^4 + gu^3 - (2R - \omega_0 Q)u^2 + 2Su - Q^2\right) \\ &= \frac{\omega_0^2}{4}(M-u)(u-m)(u-Z_1)(u-Z_2). \end{aligned} \tag{23}$$

By comparing the coefficients of (23) and assuming that Q, m, and M are given, the two additional roots Z_1 and Z_2 are found as (note that a small typo in [1] has been corrected here)

$$Z_1 = \frac{1}{2}\left\{-\left(\frac{12}{\omega_0^2}g + (M+m)\right) - \sqrt{\left(\frac{12}{\omega_0^2}g + (M+m)\right)^2 + \frac{48Q^2}{\omega_0^2 mM}}\right\},$$

$$Z_2 = \frac{1}{2}\left\{-\left(\frac{12}{\omega_0^2}g + (M+m)\right) + \sqrt{\left(\frac{12}{\omega_0^2}g + (M+m)\right)^2 + \frac{48Q^2}{\omega_0^2 mM}}\right\}.$$

The total head R and the flow force S are obtained as

$$R = \frac{\omega_0 Q}{2} - \frac{\omega_0^2}{24}\left(Z_1Z_2 + mM + (M+m)(Z_1+Z_2)\right),$$

$$S = -\frac{\omega_0^2}{24}\left((M+m)Z_1Z_2 + mM(Z_1+Z_2)\right).$$

Following the work in [1] there are two cases depending on the sign of ω_0. If $\omega_0 > 0$, then u'^2 has no singularities and there is a smooth periodic solution if $Z_2 < m < M$. If $\omega_0 < 0$, then u'^2 has two singularities and the parameter space is more restricted. To find the conditions for smooth solutions to exist, we let $\mathcal{F}(u)$ be expressed as

$$\mathcal{F}(u) = \left(Q + \frac{\omega_0}{2}u^2\right)^2 = \frac{\omega_0^2}{4}(u-A_+)^2(u-A_-)^2, \tag{25}$$

which reveals that the derivative is singular when u takes the values $A_+ = \sqrt{\frac{2Q}{-\omega_0}}$ and $A_- = -\sqrt{\frac{2Q}{-\omega_0}}$. In the case $\omega_0 < 0$, smooth solutions exist when $M < A_+$. To better understand this condition, we introduce the non-dimensional Froude number

$$F = \frac{\omega_0 M^2}{2Q}.$$

Substituting F for ω_0 we find four cases:

$$\begin{cases} 0 < F: & \text{smooth solutions exist is } Z_2 < m < M, \\ -1 < F < 0: & \text{smooth solutions exist,} \\ F = -1: & \text{limiting case of smooth solutions ceasing to exist,} \\ F < -1.1: & \text{smooth solutions do not exist but overhanging waves are possible.} \end{cases} \tag{26}$$

Only solutions of the first two cases above are seen in [1]. Below we show one representative example of each of the cases. As in [1], we use the parameters

$$g = 9.81;\ \rho = 1;\ m = 1.1;\ Q = 1.2\sqrt{g};\ h_0 = \sqrt[3]{g^{-1}Q^2};\ \omega_0 = \frac{2QF}{M^2}. \tag{27}$$

For the following figures, we use the following parameters:

$$\begin{cases} 0 < F: & M = 1.3 \text{ and } F = 1.15, \\ -1 < F < 0: & M = 1.7 \text{ and } F = -0.3, \\ F = -1: & M = 1.7 \text{ and } F = -1, \\ F < -1.1: & M = 1.7 \text{ and } F = -1.1. \end{cases}$$

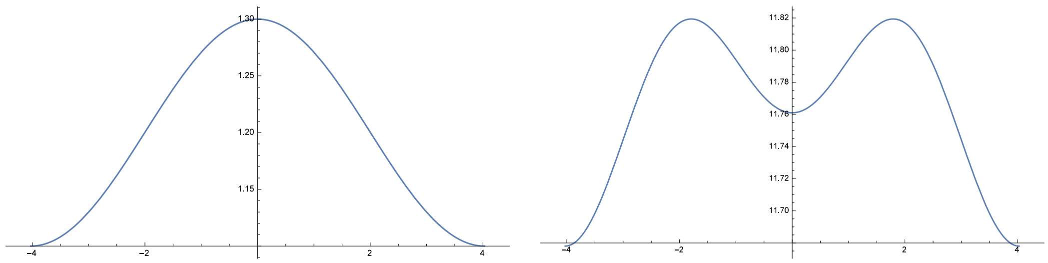

(a) (b)

Figure 2: (a) $u(x)$ as a function of x. (b) $P(u(x),0)$ as a function of x.
$0 < F$, $M = 1.3$, $F = 1.15$, and $-1/2 \leq s \leq 1/2$. Smooth solutions exist.

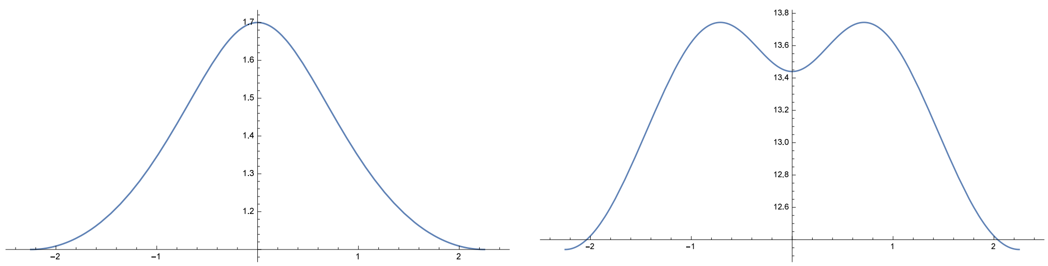

(a) (b)

Figure 3: (a) $u(x)$ as a function of x. (b) $P(u(x),0)$ as a function of x.
$-1 < F < 0$, $M = 1.7$, $F = -0.3$, and $-1/2 \leq s \leq 1/2$. Smooth solutions exist.

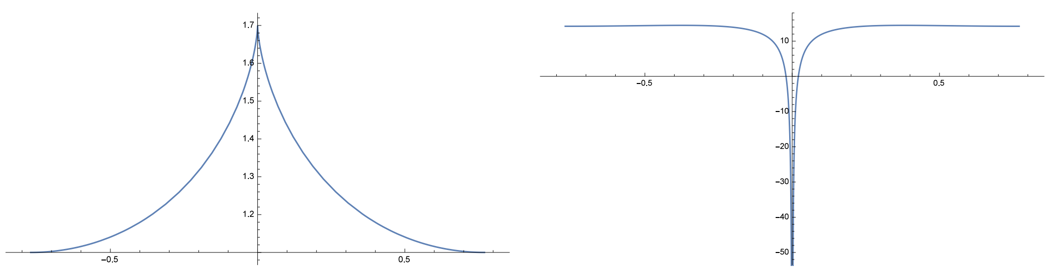

(a) (b)

Figure 4: (a) $u(x)$ as a function of x. (b) $P(u(x),0)$ as a function of x.
$F = -1$, $M = 1.7$, $F = -1$, and $-1/2 \leq s \leq 1/2$. Cusp solution.

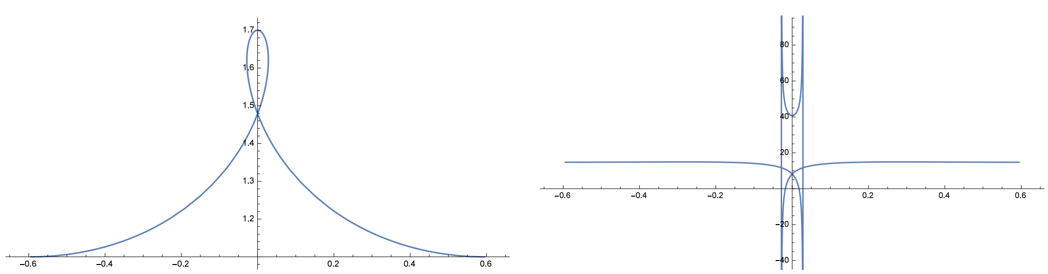

(a) (b)

Figure 5: (a) $u(x)$ as a function of x. (b) $P(u(x),0)$ as a function of x.
$F < -1$, $M = 1.7$, $F = -1.1$, and $-1/2 \leq s \leq 1/2$. Overhanging solutions.

Additionally, in order to obtain periodic solutions with $m < u(x) < M$ and with zero imaginary part, we need to set

$$c_0 = 4\omega_2(g_2, g_3), \tag{28}$$

where ω_2 is a Weierstraß half period corresponding to the lattice invariants g_2 and g_3 with non-zero imaginary part.

We produce plots of the explicit solutions for the various cases of (26) with the parameters given in (27), (28) and (32). Two plots for each case will be shown:

1. $u(x)$ as a function of x,
2. $P(u(x), 0)$ as a function of x.

Note that since our solutions are symmetric under spacial translations (varying x_2) we can shift the waves so they coincide with those in [1]. Figures 2 and 3 show two curves found in [1], and no visual difference can be detected between the explicit solutions and the numerical approximations of [1]. We notice that $x(s)$ is a monotone function of s as $F > -1$ decreases up until the critical value of $F = -1$. Beyond the critical point where $F = -1$, $x(s)$ is no longer monotone and as a result the solutions are no longer smooth. Figure 4 shows the limiting case of a cusped solution. Note that the evaluation of the pressure at the bottom under the wavecrest appears to yield extremely low and apparently non-physical values. Figure 5 shows a looped (or self-intersecting) solution which is allowed in equations (10) and (11), but not possible in (1). Since it was assumed in the derivation that the free surface is a single-valued function of x, the solution shown in Figure 5 is beyond the physical validity of the equation.

Next we investigate whether the solutions of (1) are close to the solutions of the full Euler equations with a background shear flow found in [31]. Figure 6 and 7 show a sequence of large waveheight solutions with waveheight $H = 1.2$, and for the set of parameters $g = 9.81, \rho = 1.0, h_0 = 1.0$. Note also that by rearranging the variables, we can make the self-intersecting solution look like an overhanging solution. Even though the curves shown in Figure 7 look similar to the free surface profiles shown in Figure 6 of [31], strictly speaking, the curves in Figure 7 do not represent solutions of (1).

We can also set our solutions to be 2π periodic. For this we need to examine the periods of $x(s)$ and $u(s)$. Let ω_1 be the Weierstraß half period corresponding to the lattice invariants g_2 and g_3 with non-zero real part. We note that

$$u(s + T_u) = u(s),$$

where

$$T_u = 8\omega_1,$$

denotes the period of $u(x)$, since both $\wp((s + c_0)/4; g_2, g_3)$ and $\wp'((s + c_0)/4; g_2, g_3)$ are periodic of period $8\omega_1$. Next we notice that

$$x(s + T_u) = x(s) + T_x,$$

where

$$T_x = QT_u + 2\omega_0 \left[J(m_1, n_1)J_2(\alpha) + K(m_1, n_1)J_1(\alpha) + J(n_1, m_1)J_2(\beta) + K(n_1, m_1)J_1(\beta)\right],$$

with

$$J_1(\gamma) = \frac{1}{\wp'(\gamma)} \left(-4\zeta(\omega_1)\gamma + 4\omega_1\zeta(\gamma)\right),$$

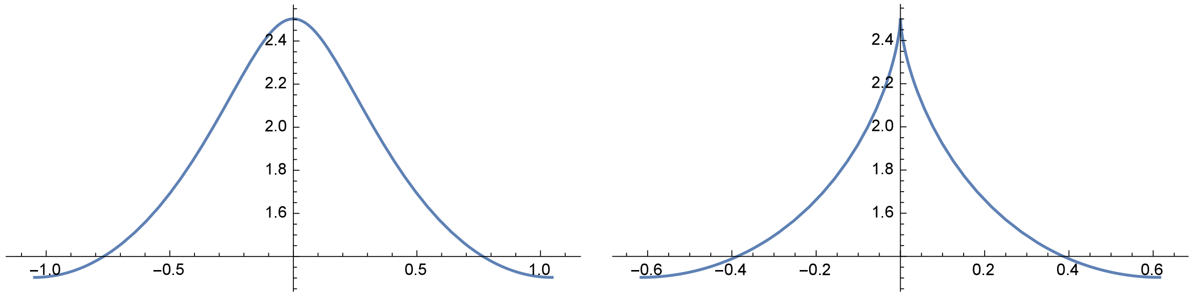

(a) (b)

Figure 6: $u(x)$ as a function of x: (a) smooth solution $F=-0.5$, (b) peaked solution $F=-1.0$.

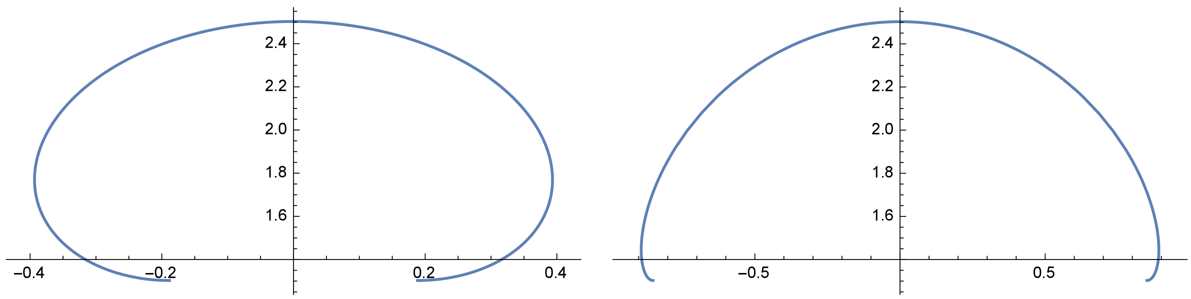

(a) (b)

Figure 7: $u(x)$ as a function of x: (a) overhanging solution $F=-2.0$, (b) overhanging solution $F=-3.0$.

and

$$J_2(\gamma)=\frac{\wp''(\gamma)}{\wp'^3(\gamma)}4\zeta(\omega_1)\gamma-\frac{4\zeta(\omega_1)}{\wp'^2(\gamma)}-2\omega_1\left(\frac{2\wp(\gamma)}{\wp'^2(\gamma)}+\frac{2\wp''(\gamma)\zeta(\gamma)}{\wp'^3(\gamma)}\right).$$

This was determined by noting that

$$I_1(u+2\omega_1,\gamma)=I_1(u,\gamma)+J_1(\gamma),$$
$$I_2(u+2\omega_1,\gamma)=I_2(u,\gamma)+J_2(\gamma),$$

which we see from [28]:

$$\zeta(u+2\omega_1)=\zeta(z)+2\zeta(\omega_1),$$
$$\sigma(u+2\omega_1)=-e^{2\zeta(\omega_1)(u+\omega_1)}\sigma(z).$$

Here T_x gives an analytical expression for the wavelength of the solution. If we wanted to force our solutions to be 2π periodic, we could simply rescale x by $2\pi/T_x$ and u by $2\pi/T_x$ as this is the scaling symmetry of (1).

In order to better compare our results with those in [1], we would like to have the peak of the wave at $x=0$. To achieve this we determine the value of s for which $u(s)$ is at a peak and call this value T_s. Taking (11) we have

$$\wp((T_s+c_0)/4,g_2,g_3)=\frac{4(-QM^2\omega_0+2RM^2+6Q^2-6SM)}{M^2},$$

where we plugged in $y=M$ and $dy/ds=0$ to be at the peak of the wave. This gives

$$T_s=4\wp^{-1}\left(\frac{4(-QM^2\omega_0+2RM^2+6Q^2-6SM)}{M^2},g_2,g_3\right)-c_0.$$

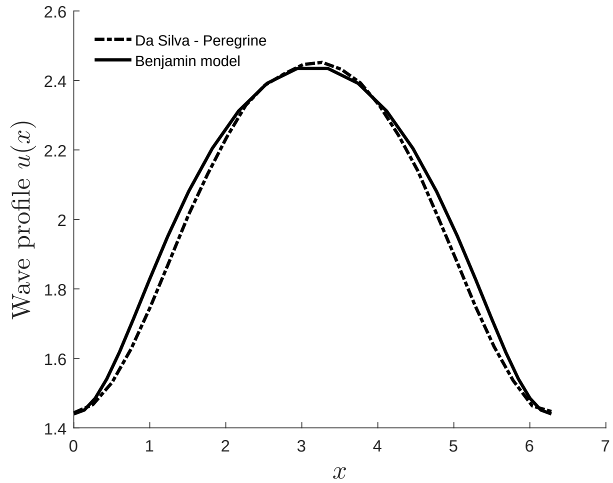

Figure 8: Comparing approximate solutions of the full Euler equations (dashed curve) to exact solutions of (1) (solid curve). The waves have waveheight $H = 1$ and wavelength 2π. The problem is normalized with $g = 1$ and $h_0 = 1$, and the background vorticity is $\omega_0 = -3$.

Thus for solutions with the peak at $x = 0$, we rewrite (17), (19), and (21) as

$$\begin{cases} y = u(T_u(s - T_s)), & \text{given in (12)}, \\ x = x(T_u(s - T_s)), & \text{given in (16)}, \end{cases} \tag{29}$$

$$\begin{cases} y = P(u(T_u(s - T_s)), z), & \text{given in (18)}, \\ x = x(T_u(s - T_s)), & \text{given in (16)}. \end{cases} \tag{30}$$

$$\begin{cases} y = \psi(u(T_u(s - T_s)), z), & \text{given in (20)}, \\ x = x(T_u(s - T_s)), & \text{given in (16)}. \end{cases} \tag{31}$$

Additionally, we set

$$\begin{aligned} x_2 = T_u \Bigg(& Q(\tilde{s} + c_0) + \omega_0 B \Bigg[\frac{8(2A - CD) \arctan\left(\frac{D + 2\wp((\tilde{s}+c_0)/4)}{\sqrt{-D^2+4E}}\right)}{(-D^2 + 4E)^{3/2}} \\ & + \frac{-4AD + 8CE + (-8A + 4CD)\wp((\tilde{s} + c_0)/4)}{(D^2 - 4E)(\wp((\tilde{s} + c_0)/4)^2 + D\wp((\tilde{s} + c_0)/4) + E)} \Bigg] \\ & + 2\omega_0 \big[J(m_1, n_1) I_2((\tilde{s} + c_0)/4, \alpha) + K(m_1, n_1) I_1((\tilde{s} + c_0)/4, \alpha) \\ & + J(n_1, m_1) I_2((\tilde{s} + c_0)/4, \beta) + K(n_1, m_1) I_1((\tilde{s} + c_0)/4, \beta) \big] \Bigg), \end{aligned} \tag{32}$$

where $\tilde{s} = T_u(0 - T_s)$. This x_2 is chosen so that when $s = 0$, $x = 0$. Additionally, note that we scale s by T_u. The scaling of s is so that as s ranges from $-1/2$ to $1/2$, we plot exactly one period of wavelength T_x.

We compare some wave profiles presented in Fig. 6 of by Teles da Silva and Peregrine [31] with solutions of same parameters computed by the current explicit method. Note that in [31], the parameters g and h_0 were normalized, so that we need to choose $g = 1$ and $h_0 = 1$.

We first present a comparison of a traveling wave of waveheight $H = 1$ and vorticity $\omega_0 = -3$. In order to get a good match with the plot from Fig. 6 of [31], we selected $m = 1.44, M =$

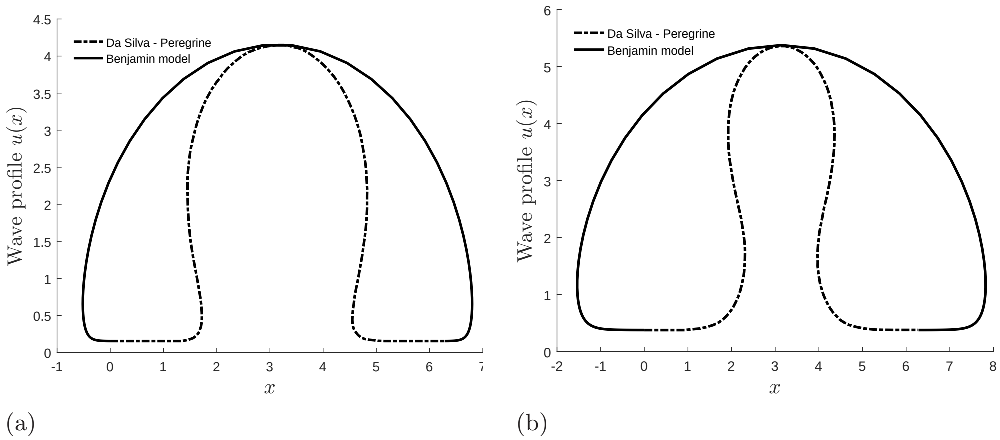

Figure 9: Comparing approximate solutions of the full Euler equations (dashed curve) to exact solutions of (1) (solid curve). The problem is normalized with $g = 1$, $h_0 = 1$ and wavelength 2π. The background vorticity is $\omega_0 = -3$. (a) waveheight $H = 4$. (b) waveheight $H = 5$.

$2.44, Q = 0.09$ Figure 8 shows an explicit solution of (1) compared to a solution of the full Euler equations shown in Fig. 6 in [31]. Even though the waveheight-depth ratio of 1/2 is not very small, the profiles match fairly closely.

Comparing higher-amplitude waves is more difficult since the solutions shown in [31] with waveheight larger than 1 are overhanging. Setting all parameters correctly yields the comparison shown in Figure 9. As can be seen, the wavelength matches, and the solutions of (7),(8) are also overhanging, but look very different nevertheless. One may conclude from this last comparison, that if solutions of (7),(8) are not single-valued, and therefore are beyond the validity of (1), they will not in general represent the physical reality of the surface-water wave problem.

4 Pressure contours and streamlines

In this section, we explore the flow underneath the surface as predicted by (1), with the help of the expression (18) for the pressure and (20) for the streamfunction.

First, pressure contours and streamlines are reviewed for positive Froude numbers F. This case corresponds to the case labelled 'upstream' in [31]. As mentioned in that work, it is in this case that a critical layer is possible. Examining figures 10-15, it appears that as the strength of the vorticity increases, first, the pressure becomes non-monotone (Figure 11). In other words, the pressure strongly departs from hydrostatic pressure, the bottom pressure is maximal under the sides of the wave (not the crest), and this goes hand in hand with the development of closed streamlines (Figure 12). For large enough Froude numbers, a critical layer (i.e., a closed circulation) develops in the interior of the fluid domain (Figure 13). In the extreme case of $F = 3$, pressure inversion occurs as regions of high pressure are above regions of low pressure in the fluid column (Figure 15).

For negative Froude numbers, the flow corresponds to the downstream case [31]. In this case non-monotone pressures also develop, but no critical layer occurs in the fluid domain. Figures 19 and 20 show strongly non-monotone pressures. Apparently, as the shape of the free surface approaches a cusped profile, non-physical features appear in the description of the flow.

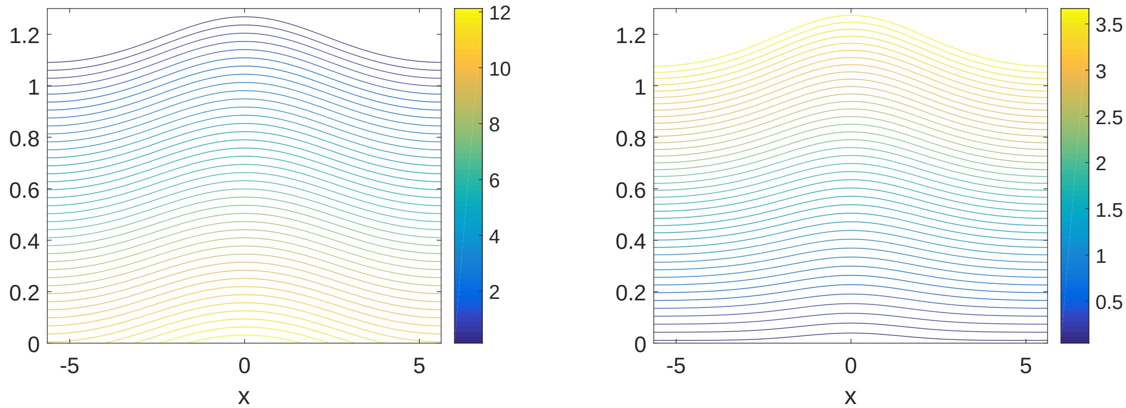

Figure 10: Traveling wave with $m = 1.1$, $M = 1.3$, and $F = 0.2$. Left: pressure contours. Right: streamlines.

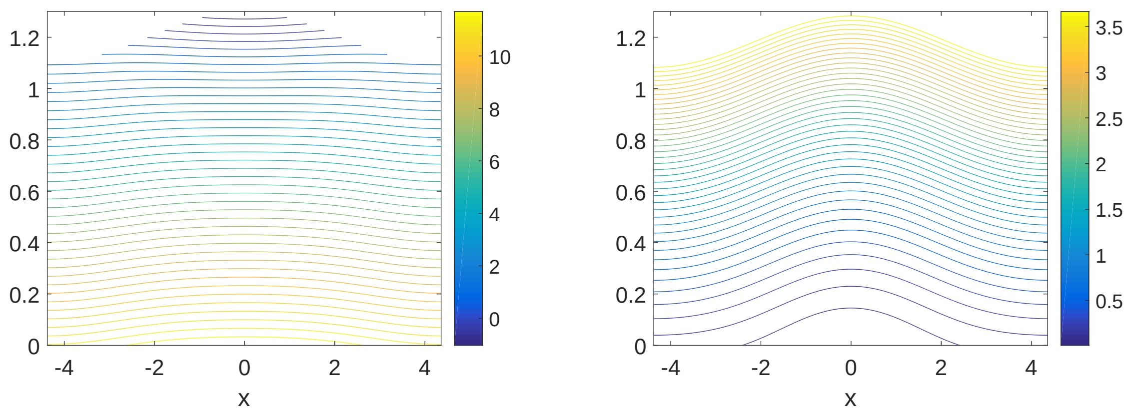

Figure 11: Traveling wave with $m = 1.1$, $M = 1.3$, and $F = 0.9$. Left: pressure contours. Right: streamlines.

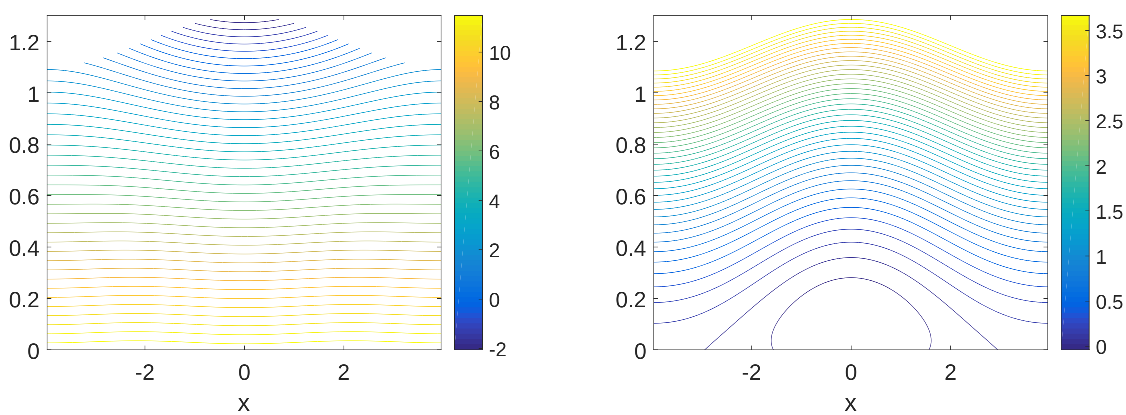

Figure 12: Traveling wave with $m = 1.1$, $M = 1.3$, and $F = 1.2$. Left: pressure contours. Right: streamlines.

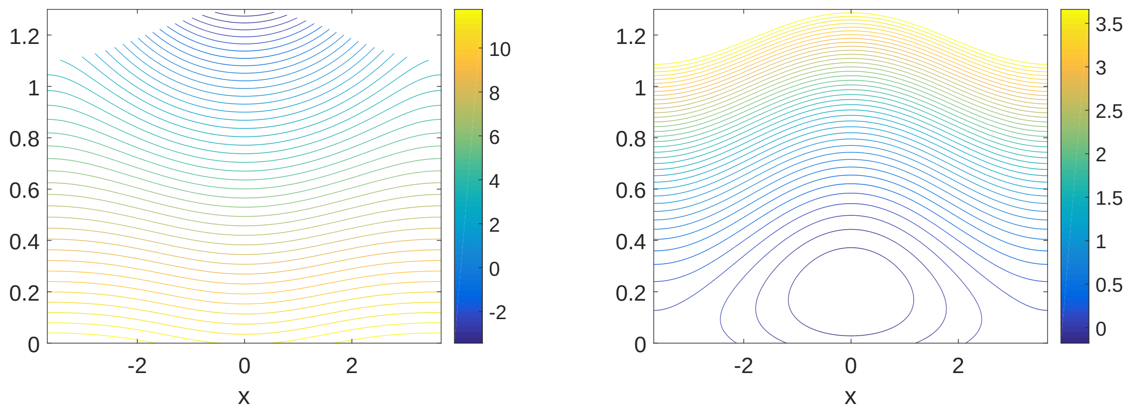

Figure 13: Traveling wave with $m = 1.1$, $M = 1.3$, and $F = 1.5$. Left: pressure contours. Right: streamlines. Pressure highly non-monotone, critical layer appears.

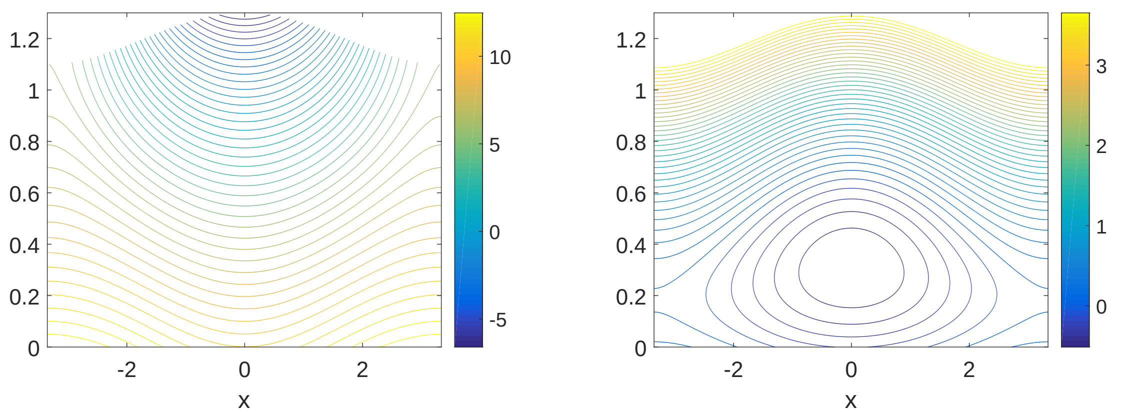

Figure 14: Traveling wave with $m = 1.1$, $M = 1.3$, and $F = 2.0$. Left: pressure contours. Right: streamlines.

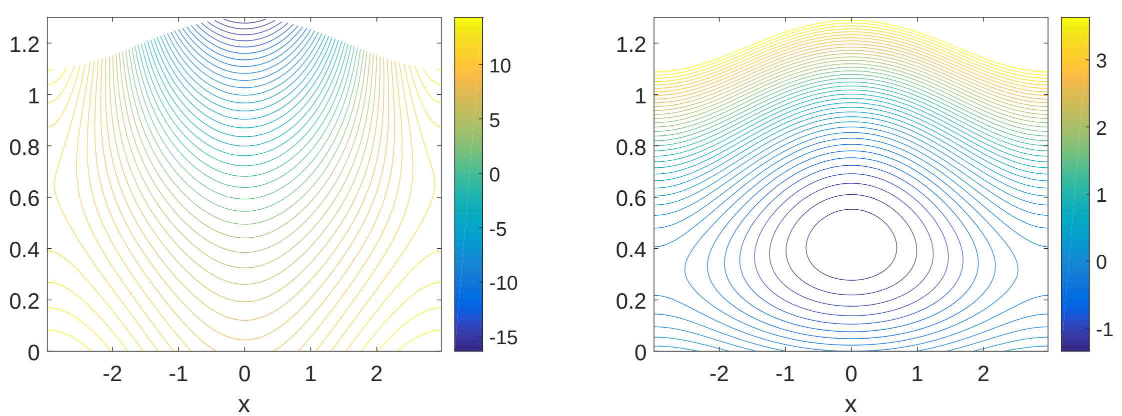

Figure 15: Traveling wave with $m = 1.1$, $M = 1.3$, and $F = 3.0$. Left: pressure contours. Right: streamlines. Pressure inversion: high pressure above low pressure.

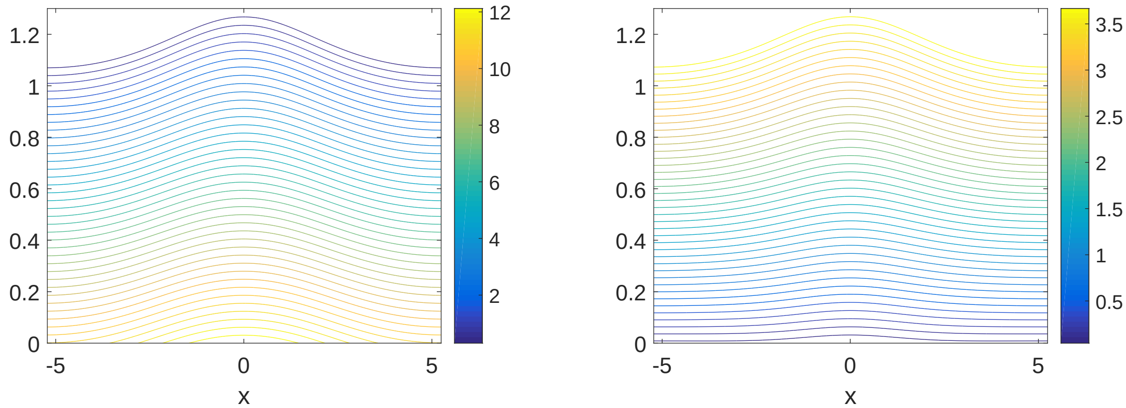

Figure 16: Traveling wave with $m = 1.1$, $M = 1.3$, and $F = -0.001$. Left: pressure contours. Right: streamlines.

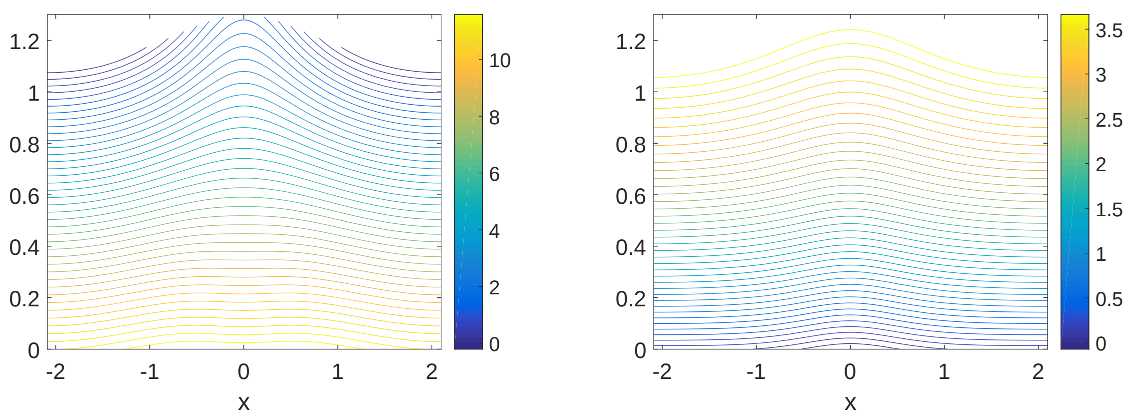

Figure 17: Traveling wave with $m = 1.1$, $M = 1.3$, and $F = -0.5$. Left: pressure contours. Right: streamlines.

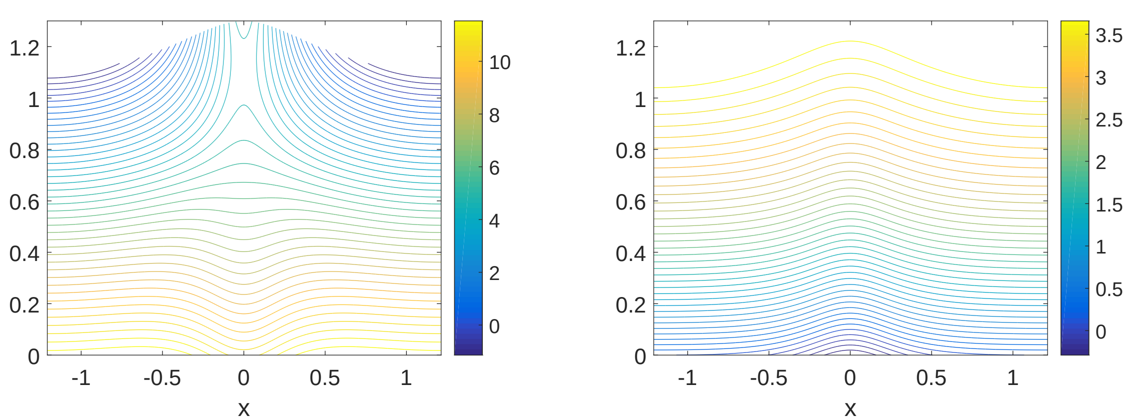

Figure 18: Traveling wave with $m = 1.1$, $M = 1.3$, and $F = -0.7$. Left: pressure contours. Right: streamlines.

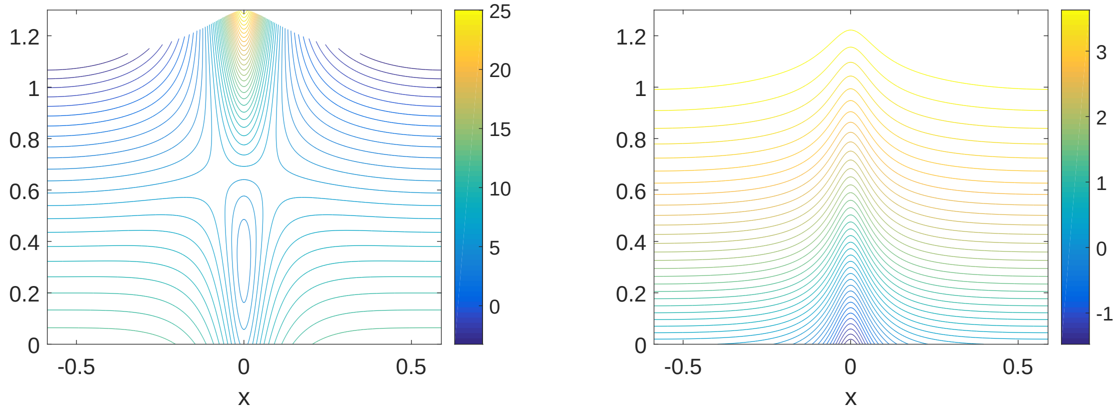

Figure 19: Traveling wave with $m = 1.1$, $M = 1.3$, and $F = -0.9$. Left: pressure contours. Right: streamlines.

5 Conclusion

The nonlinear differential equation (1) is known to be a model for steady surface water waves on a background shear flow. The equation has been found to admit solutions given explicitly in terms of a parametric representation featuring the Weierstraß P, zeta and sigma functions. This representation is a convenient tool for obtaining a variety of wave profiles without having to resort to numerical approximation. In connection with the reconstruction of the pressure underneath the surface explained in [1], and the reconstruction of the streamfunction detailed in the appendix, a complete description of the flow can be obtained.

The exact solutions of (1) have been compared to wave profiles obtained from full Euler computations in [31], and fair agreement was found for regular waves. On the other hand, overhanging waves were found not to agree with the full Euler solutions. This is not surprising since the parametric representation enables the description of multi-valued profiles which transcends the collection of solutions of (1).

With a view towards the flow in the fluid column below the wave, a number of wave shapes with increasing strength of vorticity were exhibited. It was found in the case of steady waves propagating upstream that the flow underneath the waves may feature critical layers and non-monotone pressure profiles. In the case of waves propagating downstream, the development of cusped surface profiles goes hand in hand with unrealistic pressure profiles apparently conflicting with the long-wave approximation which is the basis for the model (1). Building on the results of this paper, future work may focus on detailed comparisons of the fluid flow as described by the methods of the current work to numerical approximations of the flow governed by the Euler equations with background vorticity. Such a study will cast more light on the limitations of the current model, especially as regarding the ability to describe properties of the flow in the bulk of the fluid.

Acknowledgments

This research was supported in part by the Research Council of Norway under grant 213474/F20 and by the National Science Foundation under grant NSF-DMS-1008001. Any opinions, findings, and conclusions

or recommendations expressed in this material are those of the authors and do not necessarily reflect the views of the funding sources.

A Reconstruction of the streamfunction

We want to reconstruct the streamfunction $\psi(x,z)$ using the solutions u of the differential equation (1). This is done by using the ansatz

$$\psi = \frac{1}{2}z^2\omega_0 + zf - \frac{1}{3!}z^3 f'', \tag{33}$$

for the streamfunction and the identity

$$Q = \frac{1}{2}u^2\omega_0 + \zeta f - u^3\frac{1}{6}f'',$$

both of which are valid to second order in the long-wave parameter $\beta = h_0^2/\lambda^2$, where h_0 is the undisturbed depth of the fluid, and λ is the wavelength. To obtain an expression for f in terms of ζ, one has to invert the operator $1 - \frac{1}{6}\zeta^2\partial_{xx}$, leading to

$$\left[1 - \frac{1}{6}\zeta^2\partial_{xx}\right]^{-1}\left(\frac{Q}{\zeta} - \frac{1}{2}\zeta\omega_0\right) = f.$$

In order to bring out the difference in scales between the undisturbed depth h_0 and the wavelength L, we use the scaling

$$\tilde{x} = \frac{x}{L}, \quad \tilde{z} = \frac{z}{h_0}, \quad \tilde{\zeta} = \frac{\zeta}{h_0}, \quad \tilde{\psi} = \frac{1}{c_0 h_0}\psi, \quad \tilde{\omega}_0 = \frac{h_0}{c_0}\omega_0,$$

In addition, Q is scaled as

$$\tilde{Q} = \frac{Q}{h_0 c_0}.$$

In non-dimensional variables, the expression for ψ is

$$\tilde{\psi} = \frac{1}{2}\tilde{z}^2\tilde{\omega}_0 + \tilde{z}\tilde{f} - \frac{\beta}{3!}\tilde{z}^3\tilde{f}'' + \mathcal{O}(\beta^2).$$

The function $\tilde{f}$ is written as

$$\begin{aligned}\tilde{f} &= \left[1 + \frac{\beta}{6}\tilde{u}^2\partial_{\tilde{x}}^2 + \mathcal{O}(\beta^2)\right]\left(\frac{\tilde{Q}}{\tilde{u}} - \frac{1}{2}\tilde{u}\omega_0\right) + \mathcal{O}(\beta^2). \\ &= \frac{\tilde{Q}}{\tilde{u}} - \frac{1}{2}\tilde{u}\tilde{\omega}_0 + \frac{\beta}{3}Q\frac{(\tilde{u}')^2}{\tilde{u}} - \frac{\beta}{6}Q\tilde{u}'' - \frac{\beta}{12}\omega_0\tilde{u}^2\tilde{u}'' + \mathcal{O}(\beta^2).\end{aligned}$$

The second derivative is

$$\tilde{f}'' = 2\frac{\tilde{Q}}{\tilde{u}^3}(\tilde{u}')^2 - \frac{\tilde{Q}}{\tilde{u}^2}\tilde{u}'' - \frac{1}{2}\omega_0\tilde{u}'' + \mathcal{O}(\beta).$$

Putting these together, we find the streamfunction in terms of $\tilde{u}$:

$$\begin{aligned}\tilde{\psi} &= \frac{1}{2}\tilde{z}^2\tilde{\omega}_0 + \tilde{z}\left[\frac{\tilde{Q}}{\tilde{u}} - \frac{1}{2}\tilde{u}\tilde{\omega}_0 + \frac{\beta}{3}Q\frac{(\tilde{u}')^2}{\tilde{u}} - \frac{\beta}{6}Q\tilde{u}'' - \frac{\beta}{12}\omega_0\tilde{u}^2\tilde{u}''\right] \\ &\quad -\frac{\beta}{3!}\tilde{z}^3\left[2\frac{Q}{\tilde{u}^3}(\tilde{u}')^2 - \frac{Q}{\tilde{u}^2}\tilde{u}'' - \frac{\omega_0}{2}\tilde{u}''\right] + \mathcal{O}(\beta^2).\end{aligned}$$

References

[1] A. Ali and H. Kalisch, *Reconstruction of the pressure in long-wave models with constant vorticity* Eur. J. Mech. B Fluids **37** (2013), 187–194.

[2] A. Ali and H. Kalisch, *On the formulation of mass, momentum and energy conservation in the KdV equation*, Acta Appl. Math. **133** (2014), 113–131.

[3] T. B. Benjamin, *The solitary wave on a stream with an arbitrary distribution of vorticity*, J. Fluid Mech. **12** (1962), 97–116.

[4] T. B. Benjamin and M. J. Lighthill, *On cnoidal waves and bores*, Proc. Roy. Soc. London Ser. **A** **224** (1954), 448–460.

[5] H. Borluk and H. Kalisch, *Particle dynamics in the KdV approximation*, Wave Motion **49** (2012), 691–709.

[6] P.F. Byrd and M.D. Friedman, Handbook of elliptic integrals for engineers and scientists, vol. 67. (Springer Berlin, 1971).

[7] T.L. Clarke, B. Lesht, R.A. Young, D.J.P. Swift and G.L. Freeland, *Sediment resuspension by surface-wave action: An examination of possible mechanisms*, Marine Geology, **49** (1982) 43–59

[8] T. Colin, F. Dias and J.-M. Ghidaglia, *On rotational effects in the modulations of weakly nonlinear water waves over finite depth*, Eur. J. Mech. B Fluids **14** (1995), 775–793.

[9] A. Constantin, M. Ehrnström and E. Wahlén, *Symmetry of steady periodic gravity water waves with vorticity*, Duke Math. J. **140** (2007), 591–603.

[10] A. Constantin and J. Escher, *Symmetry of steady periodic surface water waves with vorticity*, J. Fluid Mech. **498** (2004) 171–181.

[11] A. Constantin and W. Strauss, *Exact steady periodic water waves with vorticity*, Comm. Pure Appl. Math. **57** (2004), 481–527.

[12] A. Constantin and W. Strauss, *Pressure beneath a Stokes wave*, Comm. Pure Appl. Math. **63** (2010), 533–557.

[13] A. Constantin and E. Varvaruca, *Steady periodic water waves with constant vorticity: regularity and local bifurcation*, Arch. Ration. Mech. Anal. **199** (2011), 33–67.

[14] R. Conte and M. Musette, The Painlevé Handbook (Springer Science & Business Media, 2008).

[15] W. Choi, *Strongly nonlinear long gravity waves in uniform shear flows*, Phys. Rev. E **68** (2003), 026305.

[16] L. Debnath Nonlinear Water Waves (Academic Press, 1994).

[17] S.H. Doole, *The pressure head and flowforce parameter space for waves with constant vorticity*, Quart. J. Mech. Appl. Math. **51** (1998), 61–72.

[18] S.H. Doole and J. Norbury, *The bifurcation of steady gravity water waves in (R, S) parameter space* J. Fluid Mech. **302** (1995), 287–305.

[19] M. Ehrnström and G. Villari, *Linear water waves with vorticity: rotational features and particle paths*, J. Differential Equations **244** (2008), 1888–1909,

[20] M. Ehrnström, J. Escher and E. Wahlén, *Steady water waves with multiple critical layers*, SIAM J. Math. Anal. **43** (2011), 1436–1456.

[21] I. Gradshteyn and I. Ryzhik, Table of Integrals, Series and Products, 5th edn (Academic Press, New York, 1994).

[22] V. M. Hur, *Exact solitary water waves with vorticity*, Arch. Ration. Mech. Anal. **188** (2008), 213–244.

[23] H. Kalisch, *A uniqueness result for periodic traveling waves in water of finite depth*, Nonlinear Anal. **58** (2004), 779–785.

[24] J. Ko and W. Strauss, *Large-amplitude steady rotational water waves*, Eur. J. Mech. B Fluids **27** (2008), 96–109.

[25] P.K. Kundu and I.M. Cohen, Fluid Mechanics, 4th edition (Academic Press, 2008)

[26] Y. Li and S.Å. Ellingsen, *Ship waves on uniform shear current at finite depth: wave resistance and critical velocity*, J. Fluid Mech. **791** (2016), 539–567.

[27] C.C. Mei, S.-J. Fan and K.-R. Jin, *Resuspension and transport of fine sediments by waves*, J. Geophys. Res. Oceans **102** (1997), 15807–15821.

[28] F.W.J. Olver, D.W. Lozier, D.F. Boisvert and C.W. Clark, Eds. NIST Handbook of Mathematical Functions, (Cambridge University Press, New York, 2010).

[29] J.S. Ribberink and A.A. Al-Salem, *Sediment transport in oscillatory boundary layers in cases of rippled beds and sheet flow*, J. Geophys. Res. Oceans **99** (1994), 12707–12727.

[30] R. Thomas, C. Kharif and M. Manna, *A nonlinear Schrdinger equation for water waves on finite depth with constant vorticity* Phys. Fluids **24** (2012), 127102.

[31] A.F. Teles da Silva and D.H. Peregrine, *Steep, steady surface waves on water of finite depth with constant vorticity*, J. Fluid Mech. **195** (1988), 281–302.

[32] J. Touboul, J. Charland, V. Rey and K. Belibassakis, *Extended mild-slope equation for surface waves interacting with a vertically sheared current*, Coastal Engineering **116** (2016), 77–88.

[33] J. Touboul and E. Pelinovsky, *Bottom pressure distribution under a solitonic wave reflecting on a vertical wall*, Eur. J. Mech. B Fluids **48** (2014), 13–18.

[34] G. Valiron and J. Glazebrook, The Geometric Theory of Ordinary Differential Equations and Algebraic Functions (Math Sci Press, 1984).

[35] J.-M. Vanden-Broeck, *Periodic waves with constant vorticity in water of infinite depth*, IMA J. Appl. Math. **56** (1996), 207–217.

[36] E. Wahlén, *Steady water waves with a critical layer*, J. Differential Equations **246** (2009), 2468–2483.

[37] E. Wahlén, *Hamiltonian long-wave approximations of water waves with constant vorticity*, Phys. Lett. A **372** (2008), 2597–2602.